

Intraocular pressure remote photonic biomonitoring based on temporally encoded external sound wave stimulation

Aviya Bennett
Yevgeny Beiderman
Sergey Agdarov
Yafim Beiderman
Nisan Ozana
Michael Belkin
Zeev Zalevsky

Intraocular pressure remote photonic biomonitoring based on temporally encoded external sound wave stimulation

Aviya Bennett,^a Yevgeny Beiderman,^a Sergey Agdarov,^a Yafim Beiderman,^a Nisan Ozana,^a Michael Belkin,^b and Zeev Zalevsky^{a,*}

^aBar-Ilan University, Faculty of Engineering and the Nanotechnology Center, Ramat-Gan, Israel

^bTel-Aviv University, Goldshleger Eye Research Institute, Tel Aviv, Israel

Abstract. Continuous noninvasive measurement of intraocular pressure (IOP) is an important tool in the evaluation process for glaucoma. We present a methodology enabling high-precision, noncontact, reproducible, and continuous monitoring of IOP based on the value of the damping factor of transitional oscillations obtained at the surface of the eye after terminating its stimulation by a sound wave. The proposed configuration includes projection of a laser beam and usage of a fast camera for analyzing the temporal–spatial variations of the speckle patterns backscattered from the iris or the sclera following the above-mentioned sound waves external stimulation. The methodology was tested on an artificial eye and a carp fish eye under varying pressure as well as on human eyes. © 2018 Society of Photo-Optical Instrumentation Engineers (SPIE) [DOI: 10.1117/1.JBO.23.11.117001]

Keywords: optics; lasers; speckle; Fourier optics and signal processing; medical optics instrumentation; pattern recognition; intraocular pressure.

Paper 180261RR received May 4, 2018; accepted for publication Oct. 17, 2018; published online Nov. 15, 2018.

1 Introduction

Glaucoma^{1–6} is the second leading cause of blindness worldwide, disproportionately affecting women and Asians.¹ It could result in visual impairment and eventually irreversible blindness if left undiagnosed and untreated.^{1,5} Currently, the fundamental risk factor for glaucoma is high intraocular pressure (IOP), which is at present the only treatable risk factor,^{7–10} although there remains the ambiguity of normal tension glaucoma with “regular” IOP and ocular hypertension with elevated IOP but no disease.

IOP is a dynamic physiologic variable with regular circadian modification and random variation over short and long periods as muscle tone and the physiological condition of the subject alternate.^{11–17} Therefore, accurate monitoring of IOP is a fundamental clinical aspect of glaucoma care. Although many clinical decisions are based on IOP, current handling of glaucoma involves periodic measurement of IOP during office hours, which is a suboptimal resolution, presenting incomplete characterization of the variable nature of IOP.

Goldmann applanation tonometry (GAT) is the most commonly used ophthalmic instrument for IOP examination.¹⁸ Although GAT is very accurate,¹⁹ it is affected by inner-individual variations due to diversity in corneal thickness and rigidity while being an invasive procedure that necessitates the use of anesthetic eye drops and limiting IOP monitoring over time. It was found that biochemical cornea properties influence the accuracy of applanation tonometry.^{20,21} The ocular response analyzer^{22–25} allows adjustment of IOP taking into consideration the biomechanical properties of the cornea. An alternative way of measuring IOP is by air puff tonometer.^{26,27} The tonometer measures IOP in terms of the eye’s resistance to blown air.²⁸ The

tonometer has no invasive component, but it still involves an inability to monitor IOP over long periods of time to obtain more complete IOP profiles. The level of precision for air puff tonometer is lower than the precision obtained by GAT.

This limitation encouraged researchers to develop methods for continuous IOP monitoring. Several examples of such systems contain implants with telemetric pressure transducers,^{29–32} sensing contact lenses,^{33–38} implantable microfluidic devices,³⁹ ocular telemetry sensors,⁴⁰ and optical devices.^{41–44} Zuckerman and Grossman⁴⁵ developed a way of acquiring biological pulses and blood flow in the eye by applying an ultrasonic wave to its surface. Acka et al.⁴⁶ observed the mechanical resonance modes of the cornea agitated by sound waves. Although these techniques use sound-driven technology for measuring the eyes’ physical parameters, no correlation with IOP was found. Recently, a special laser-based setup introduced a capability to sense remote speech signals, heart beats, and vibrations from remote bodies using reflected secondary speckle patterns.^{47,48} Previous studies have shown that heartbeats,^{47,49} blood pulse pressure,⁵⁰ breast cancer,⁵¹ and blood glucose^{52,53} can be estimated remotely using a secondary speckle-based photonic system.

In the current research, we used the above technology for semicontinuous noninvasive IOP measurement. Following presentation of the basic principle,^{54,55} a technique using sound-driven corneal vibration was introduced in the current study. The existing method for detecting IOP based on a sound wave for corneal oscillation^{45,56,57} was used by us before while the reflected secondary speckle patterns variations were analyzed.

In this paper, we changed the concept of measurement by stimulating the eye with a temporally encoded external signal and after terminating the stimulation, observing transitional

*Address all correspondence to: Zeev Zalevsky, E-mail: Zeev.Zalevsky@biu.ac.il

oscillation of the surface of the eye for ~ 0.05 s. The hardware setup was changed in a way that simplified operability and allowed measurement of both artificial eyes as well as animal and human eyes.

Note that the air puff tonometer is usually used for checkup while having reduced accuracy; however, our methodology may allow frequent semicontinuous measurements at higher accuracy.

The idea of extended or semicontinuous IOP measurements is based on the assumption that future measuring device will be miniaturized. It will be mounted on special spectacles frame. Periodic stimulation of the eye by sound wave and respective measurements will allow monitoring the IOP. Preliminary calibration of the device for each individual should allow improvement in the measurement's precision.

2 Theoretical Background

2.1 Brief Background of the Proposed Technology

The proposed technology comprises from further development of IOP measurement concept based on the tracking of speckle patterns reflected from the cornea. A laser beam illuminates the agitated area and scattered light is back reflected toward a fast imaging camera. The speckles are self-interfering random patterns produced by interference of a set of wave fronts of the same wavelength with different phases and amplitudes. Speckle patterns are produced due to the roughness of the surface of the inspected tissue when illuminated by spatially and temporally coherent laser beam.

When aggregated on the detector plane, the wave-fronts provide a random intensity pattern due to the interference phenomenon, resulting in speckle patterns known as secondary or subjective speckles. The working principle underlying the suggested technology proposes not to focus the camera on the inspected tissue of the cornea, but rather on the far- or near-field such that the object itself is defocused. In doing so, the tissue's vibrations cause the speckle patterns to shift rather than change in time, with the shift being proportional to the extent of tilting of the illuminated surface. These transversal shifts can be traced by a correlation-based algorithm over the recorded images. The information obtained by image correlation is directly related to the surface tilting movement.

2.2 Underlying Principle of the Proposed Method for IOP Monitoring

The theoretical background of the optical setup lies in detection of the tilting movement using a laser and a defocused fast camera to transform this movement into a transversal shift of the speckle patterns. The requirement for focal length F of the camera is Ref. 47:

$$F = \frac{K\Delta x Z_3 D}{Z_2 \lambda}, \quad (1)$$

where Δx is the size of the pixel in the detector, Z_3 is the distance between the secondary speckle and the imaging module, Z_2 is the distance between the illuminated surface and the secondary speckle (due to defocusing), λ is the laser wavelength, D is the laser spot diameter, K is the minimum number of pixels by which it is assumed that every speckle in this plane will be seen.

Z_2 needs to fulfill the far-field approximation:

$$Z_2 > \frac{D^2}{4\lambda}. \quad (2)$$

The previous works related to speckle-based tracking technology were focused on evaluation of the cornea vibration amplitude under different internal pressures applied to a rabbit eye. The criteria of evaluation were the amplitude of corneal self-vibration. It was found that IOP is correlated to the vibration amplitude; however, the measured amplitude of the vibration depends on the position of the laser beam on the corneal surface.^{54,55} To minimize such constrain, we found it necessary to introduce physical parameters of the corneal vibration giving more consistent results. For this purpose, the corneal surface was agitated by sound wave and damped oscillation of the cornea was evaluated as a function of IOP.

2.3 Q factor of Damped Oscillation

The Q factor is a dimensionless parameter that indicates energy losses within the vibrating element during damped oscillation. We propose an innovative methodology for evaluating IOP from the relationship between the Q factor and the IOP. To measure the Q factor, a periodic sound wave was made to agitate the eye surface for a few seconds and was then turned off. During the transition period when the sound wave dissipated, the eye surface was still stimulated by the damped signal and continued to oscillate with a frequency close to the stimulation frequency [see Fig. 1(a)]. The Q factor was calculated for the temporal interval between the overshoot and the average noise level [see Fig. 1(b)]. Overshoot refers to the transitory values of any parameter that exceeds its steady state.⁴⁶ The automatic calculation algorithm for the Q factor was developed in MATLAB.

The differential equation for the forced harmonic oscillator applied for the evaluation of the Q factor is Ref. 58:

$$F(t) = m \frac{d^2 x}{dt^2} + \gamma m \frac{dx}{dt} + m\omega_0^2 x, \quad (3)$$

where F is the external agitation force, m is the object's mass, x is the position of the object with respect to the equilibrium position, t is the time, γ is the damping coefficient of the cornea, and ω_0 is its resonant frequency. In case of corneal stimulation by periodic acoustic pressure, $F(t)$ could be described as follows:

$$F(t) = F_0 \cos(\omega t), \quad (4)$$

where F_0 is the pressure maximum and ω is the frequency of the forced oscillation.

For the transition period when the acoustic source is switched off and oscillation continues for a short period:

$$F(t) = F_0 e^{-\beta t} \cos(\omega t), \quad (5)$$

where β is the damping coefficient of the acoustic source.

Movement in the x -direction for the transition from steady state to a condition where $F(t) = 0$ could be described as follows Ref. 58:

$$x = \rho F_0 e^{-\beta t} \cos(\omega t + \theta), \quad (6)$$

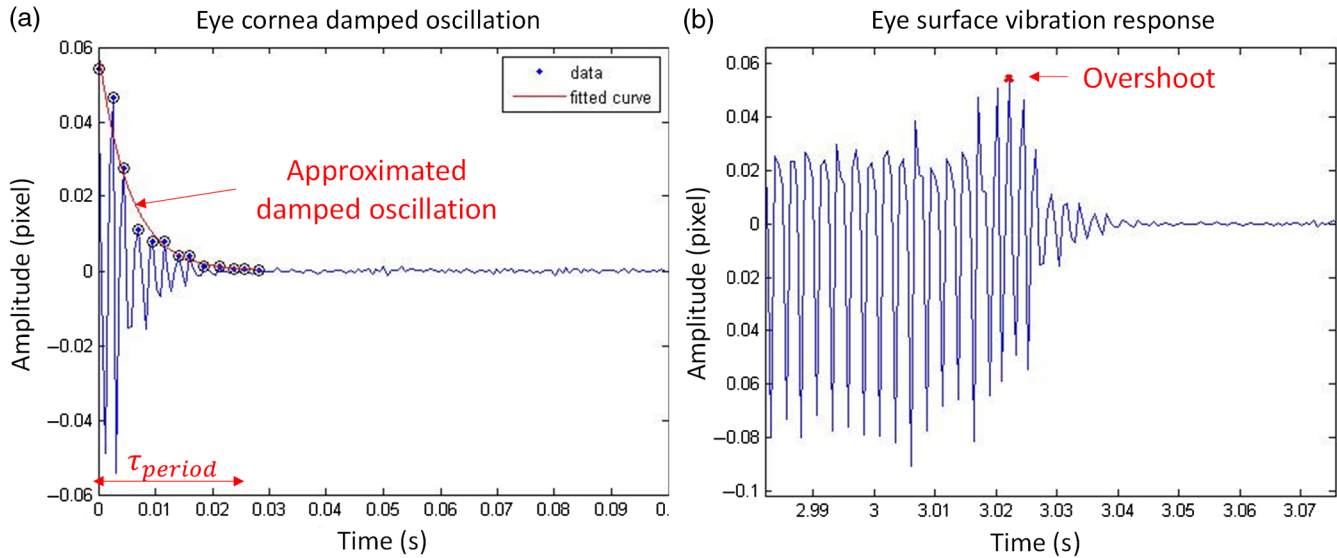


Fig. 1 Illustration of oscillation terms. (a) Artificial eye approximated damped oscillation and (b) artificial eye vibration response signal.

where θ is the phase shift between the agitation force and the output signal.

Coefficient ρ could be written as

$$\rho = \frac{1}{m\sqrt{[(\omega^2 - \omega_0^2)^2 + \gamma^2\omega^2]}}. \quad (7)$$

In our case, $\omega \gg \omega_0$ and Eq. (7) could be presented as follows:

$$\rho = \frac{1}{m\omega\sqrt{(\gamma^2 + 1)}}. \quad (8)$$

Therefore, Eq. (6) can be described as

$$x = \frac{F_0 e^{-\beta t}}{m\omega\sqrt{(\gamma^2 + 1)}} \cos(\omega t + \theta). \quad (9)$$

As before $\omega \gg \omega_0$ and therefore

$$tg\theta = \frac{\gamma}{\omega}, \quad (10)$$

where γ is the damping coefficient and ω is the frequency of the forced corneal oscillation.

From Eq. (10) follows that the phase shift between the agitation force and the eye response could also be used as a parameter for the IOP evaluation. We assumed that the cornea damping coefficient γ could be related to IOP.

In the current experiment, the IOP was evaluated as a function of the Q factor determined during the transitional period when the stimulation of the eye was stopped, see Fig. 1:

$$Q = \frac{\pi}{\delta}, \quad (11)$$

where δ is the logarithmic attenuation decrement:

$$\delta = \ln \left[\frac{\text{peak}(t)}{\text{peak}(t+T)} \right], \quad (12)$$

where t is the time and T is the damped oscillation period.

The average value of δ was evaluated as follows:

$$\delta_{\text{avg}} = \frac{1}{m-1} \sum_{n=1}^{m-1} \ln \left[\frac{\text{peak}(t)}{\text{peak}(t+T)} \right], \quad (13)$$

where m is the number of the selected damping peaks.

The Q factor was found according to

$$Q_{\text{factor}} = \frac{\pi}{\delta_{\text{avg}}}. \quad (14)$$

The model for the oscillation of the corneal surface of the human eye is more complicated than that of the artificial eye. It contains noises specific to humans, but the described physical principle and correlation between IOP and Q factor could be applied for testing of humans as well.

It should be mentioned that the variation in the eye properties between the tested individuals could also affect determination of the Q factor. In addition to further investigation of the variation of the Q factor, we are also assuming that the calibration of the measuring device for each individual before IOP monitoring will allow to increase the level of precision.

2.4 Multidimensional Model

Apart from the Q factor, we also evaluated the correlation of IOP with the spectrum of variables obtained from the measurements. It was assumed that variables such as eye vibration frequency, signal amplitude, spectral amplitude, and the area under the spectrum graph could be related to IOP. To verify this assumption, the correlation between the mentioned parameters and IOP was evaluated.

3 Experimental Setup

A sketch of the optical system and the experimental setup for artificial eye IOP measurement are shown in Fig. 2.

The setup for testing the carp fish eyes remains the same as the artificial eye setup with only the eyeball being fixed on a rigid holder.

The experimental setup for human IOP measurement is shown in Fig. 3.

The optically based monitoring device was positioned 35 cm from the tested eye (artificial eye, carp fish, or the human). As diffraction of the speckle occurred at a wide angle, there is no constraints regarding the position of the fast imaging camera.

The system contains an acoustic stimulator, laser, and fast camera for monitoring the secondary speckle patterns back reflected from the eyeball. A JDS uniphase CW 1550-nm WDM DFB laser was positioned directly opposite to the eyeball at a distance of 32 cm. The optical beam was fixed at a selected location on the cornea. The power of the infrared laser was within the safety range ($750 \mu\text{W}$) approved by European Standard EN 60825-1. The speckle patterns reflected from the cornea were analyzed using an EHD Imaging InGaAs IK1112 digital camera. The camera's focal length was 55 mm, with an F number of 2.8. The illuminating beam was 3 mm in diameter.

The cornea was stimulated by a high-fidelity loudspeaker (Pioneer Ts-G1615R) with an excitation frequency of 390 Hz@105 dB, producing the best signal-to-noise ratio from the human eye (after a sweep on frequencies between 130 and 1300 Hz on three human eyes). The speaker was controlled by an arbitrary waveform function generator (Tektronix, AFG3022B). The eyes were irradiated by the sine sound wave for three seconds before agitation was stopped. It should be mentioned that the duration of the

agitation could be varied and significantly decreased without affecting the measurements.

The frame rate of the digital camera was four times higher than the frequency measured, to be in the safe side with respect to fulfilling the Nyquist sampling ratio requirements. Each frame of the camera's output contained a secondary speckle pattern correlated to the next frame using MATLAB Software. We extracted the position of the correlation peak on each consecutive frame and used it to determine the tilting movement of the cornea surface in X - and Y -directions. The plotted output (tilting displacement in X -direction) versus time is shown in Fig. 1(b).



Fig. 3 The coauthor Sergey Agdarov demonstrates the human IOP measurement experimental setup.

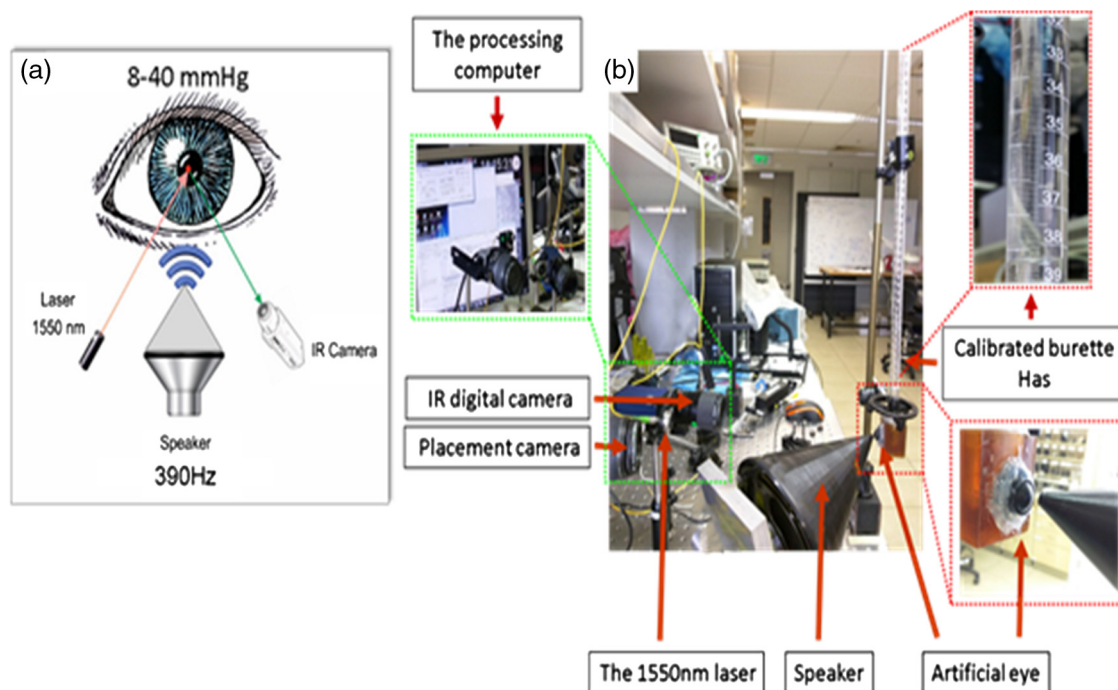


Fig. 2 Implemented optical configuration for remote measurement of IOP. (a) Sketch of the optical system and (b) the setup for the artificial eye IOP measurement.

The spectrum of the tilting oscillation signal during agitation was obtained by Fourier transform.

Note that in the near future, we intend to miniaturize the device of Fig. 3 and to mount it on a glasses frame to allow semicontinuous measurement of IOP.

4 Methods and Experimental Results

To determine the relationship between the parameters of corneal oscillation and IOP, the investigation was planned in several steps.

1. Testing of the artificial eyes under different pressures applied by a calibrated water column.
2. Testing of the carp fish eyes under different pressures applied by a calibrated water column.
3. Preliminary testing on human eyes.

Informed consent was obtained from all subjects in accordance with the Ethical Committee of the University. All research procedures were performed according to the Helsinki approval obtained from Tel Hashomer hospital.

4.1 Artificial Eye Testing

4.1.1 Q-factor

In the proposed innovative methodology, IOP was evaluated by determining its relationship with the Q factor of damped oscillation. The artificial eye was fixed to a rigid holder to minimize ambient vibration. The artificial eye pressure was controlled by connecting a burette filled with water to the eye. The eye pressure levels were selected within 8 to 40 mm with 4-mmHg steps equivalent to a 13.2-cm water column (see Fig. 4).

The measurement included 10 repetitions for each pressure. The test was performed for two eyes with different corneal thickness of 0.18 and 0.25 mm.

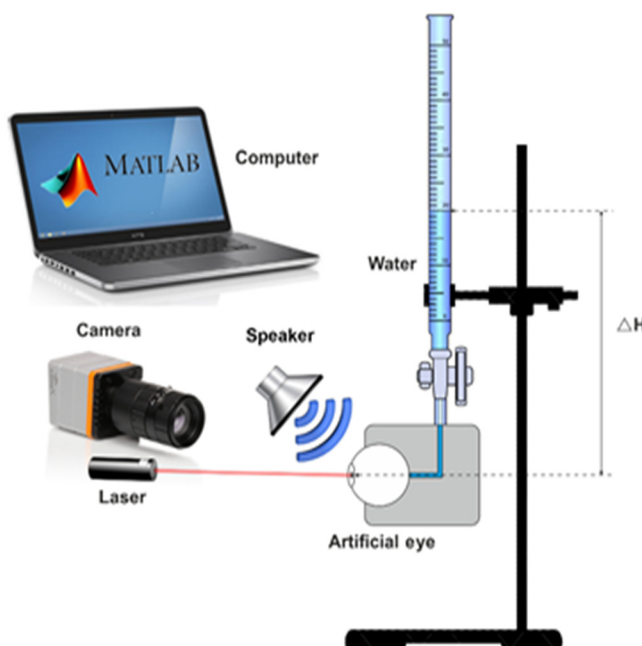


Fig. 4 The artificial eye pressure calibrated system.

The artificial eyes were selected from a Kowa Ltd. set of artificial eyes. Although thickness of artificial eyes is beyond the thickness of the human eyes being in the range of 0.46 to 0.60 mm, we considered to test the Kowa artificial eyes to evaluate the influence of the membrane thickness on the IOP measurement. An investigation into the effect of corneal thickness within the range typical for human is the aim of our next research.

Material of the artificial eye is silicon-based polymer with the following average parameters: density 1.7 t/m^3 , Poisson ratio 0.48, Young's modulus 0.025 GPa, and Elastic limit 3.4 Mpa. Average values, the coefficient of variation, and standard deviation were calculated for the above parameters to ensure that the tests were statistically significant (95% confidence interval with 10% selected margin of error). Linear and nonlinear correlation and regression analysis were applied to determine the relationship between IOP, the Q factor, and other parameters.

The relationship between IOP and the Q factor for artificial eyes is shown in Fig. 5.

4.1.2 Multidimensional linear model

We used the multidimensional linear model to evaluate the IOP as a function of the resulting parameters for 0.25-mm-thick artificial cornea. The following parameters were included in the model:

1. Q factor (Q_f).
2. Damped oscillation frequency.
3. Signal amplitude in the X (SA_x) and Y (SA_y) directions.
4. Signal spectrum [fast Fourier transform (FFT)] amplitude at the excitation frequency in the X (FFT_xH) and Y (FFT_yH) directions.
5. The area under the spectral (FFT) graph corresponding to the signal's energy in the X ($FFTaX$) and Y ($FFTaY$) directions.

The Q factor and SA_y , having a significant correlation with IOP ($r = -0.99$, -0.44 , respectively), were incorporated in the model.

The multilinear regression is shown in Eq. (15):

$$IOP_{\text{Calc}} = 70.46 - 6.08Q_f + 23.12SA_y, \quad (15)$$

where Q_f is the Q -factor and SA_y is the signal amplitude along the Y direction.

The multidimensional correlation coefficient is $R = 0.992$. Thus, it can be concluded that the difference between one-dimensional (1-D) and two-dimensional (2-D) models is not significant, so that a 1-D model based on the Q factor can also be used. The result of the actual IOP (purple bars) versus the result of the multidimensional linear regression (blue bars) is shown in Fig. 6.

4.2 Fish Eye Testing

The proposed methodology was also tested on carp fish eye. Three carp fish eye globes were acquired from a local distributor within <2 to 3 h of postmortem, and experiments were performed within 8 h of delivery. The experimental setup remained

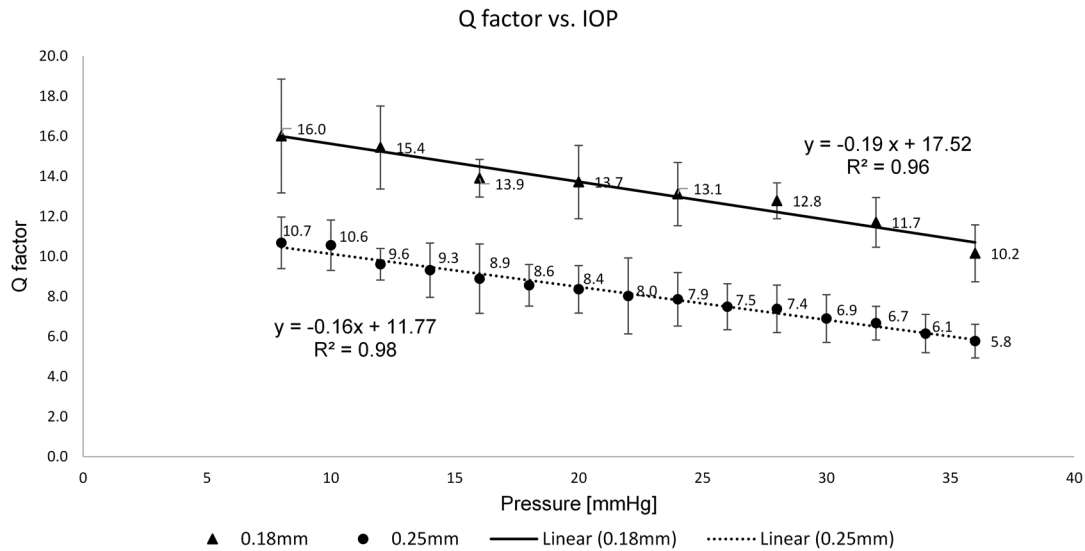


Fig. 5 The relation between Q -factor and IOP for artificial eyes having membrane thickness of 0.18 and 0.25 mm.

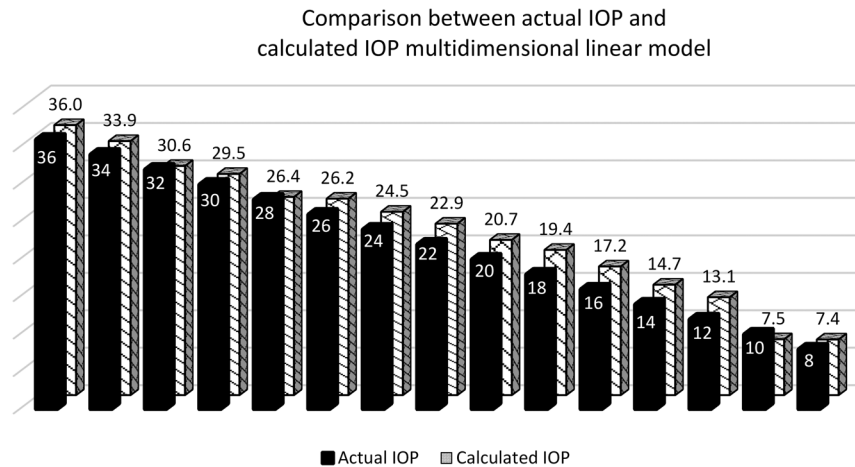


Fig. 6 Actual IOP versus calculated IOP by multiple linear regression.

the same as in Fig. 2, but to enable these measurements, the artificial eye was replaced by the carp fish eye. For proper installation and prevention of bulk movement, the eyeball was fixed on a rigid holder. The IOP level of the eyeball was controlled by using a needle inserted into the rear side of the fish eye and connected to a tap water-filled calibrated burette. The experiment was conducted under the same conditions as for the artificial eye, but the eye pressure levels were varied from 12 to 40 mm (with 4-mmHg steps) by filling the burette with tap water. The measurement included 10 repetitions. Figure 7(a) shows that the overshoot observed on the recorded signal is apparent (marked in red), while the damped oscillation area may also be observed [see Fig. 7(b)].

The relationship between the Q factor and the IOP for the tested carp fish eye is shown in Fig. 8.

The IOP model for the carp fish eye fits quadratic model compared with the artificial eye IOP model having best linear fit. However, the same decreasing trend in the relationship between the Q factor and the IOP has been observed.

4.3 Human Eyes

The current methodology was also applied for IOP measurement on human eyes. To enable these measurements, the artificial eye was removed and a chin and forehead support was added to the experimental setup to stabilize the head of a person being tested. The eye was externally stimulated by sound waves and the response was captured. In Fig. 9(a), the overshoot response in the human eye is apparent (marked in red) and the oscillation damping area may also be observed.

For the preliminary investigations, 10 individuals aged 25 to 70 years were tested. The human eyes measurements are noisier than those of the artificial eye. The recorded signal needs numerical filtering and larger number of experimental repetitions for averaging to obtain a better signal-to-noise ratio (SNR). One reason for the fact that the fish eye measurement was less noisy is that the fish eyes were tested right after extraction and fixing on a rigid holder, whereas human subjects tend to have slight movements during measurements.

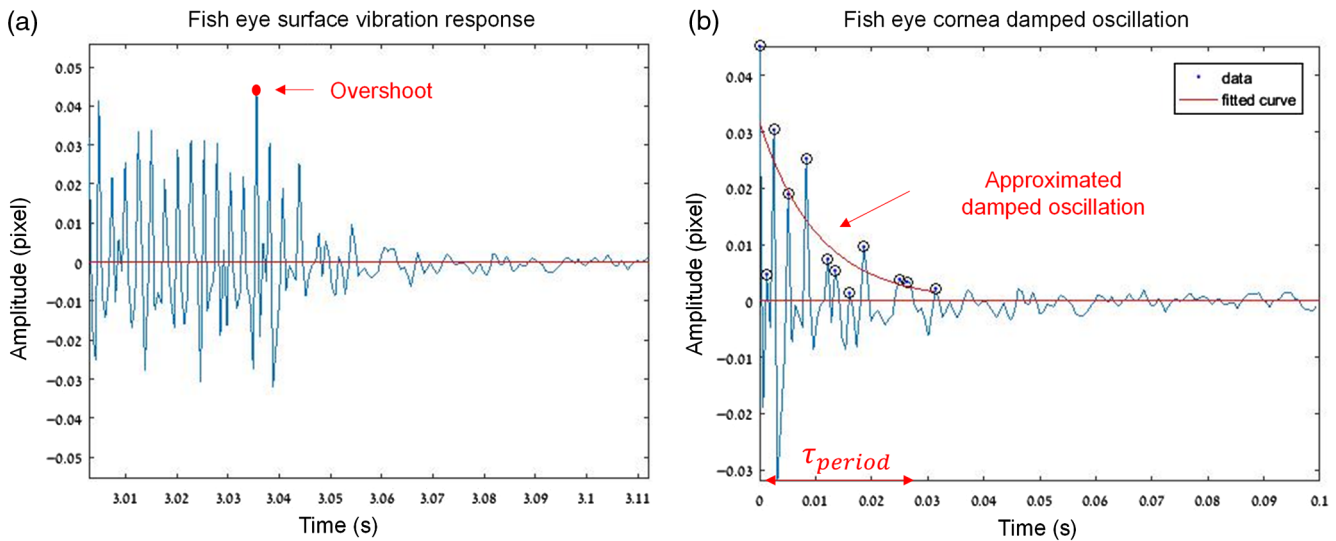


Fig. 7 Fish eyes experimental results. (a) The fish eye agitation response signal and (b) fish eye approximated damped oscillation.

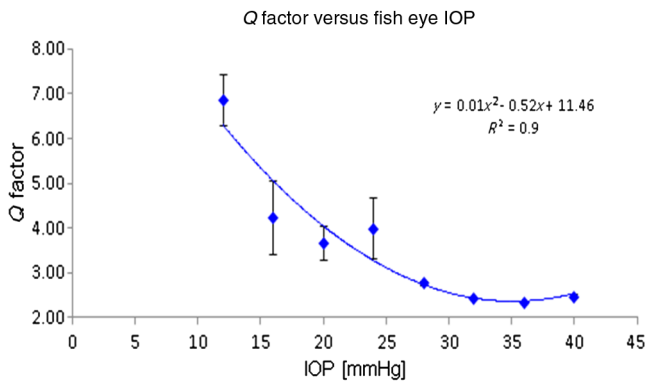


Fig. 8 The relation between the Q -factor and the IOP for carp fish eye.

Figure 9 shows that the human eye response signal is distinct, and the SNR ratio is significant. It should be mentioned that dryness of the eyes has not been evaluated during the tests. The blinking of human eyes was restricted during the tests and periods of blinking were disregarded.

Furthermore, the external excitation frequency is clearly visible in the spectrum graph in the signal as shown in Fig. 10.

In our experiments, it is important to note that the duration of the agitation could be shortened, and periodical stimulation will allow to have semicontinuous measurements as claimed in this paper, which could be sufficient for evaluation versus time.

5 Conclusions

For the first time, IOP was measured using a novel technique based on the relationship between IOP and the Q factor of damped corneal oscillation. The relationship was experimentally proven on both artificial eye and carp fish eye. The measurements, based on tracking of the temporal displacement of

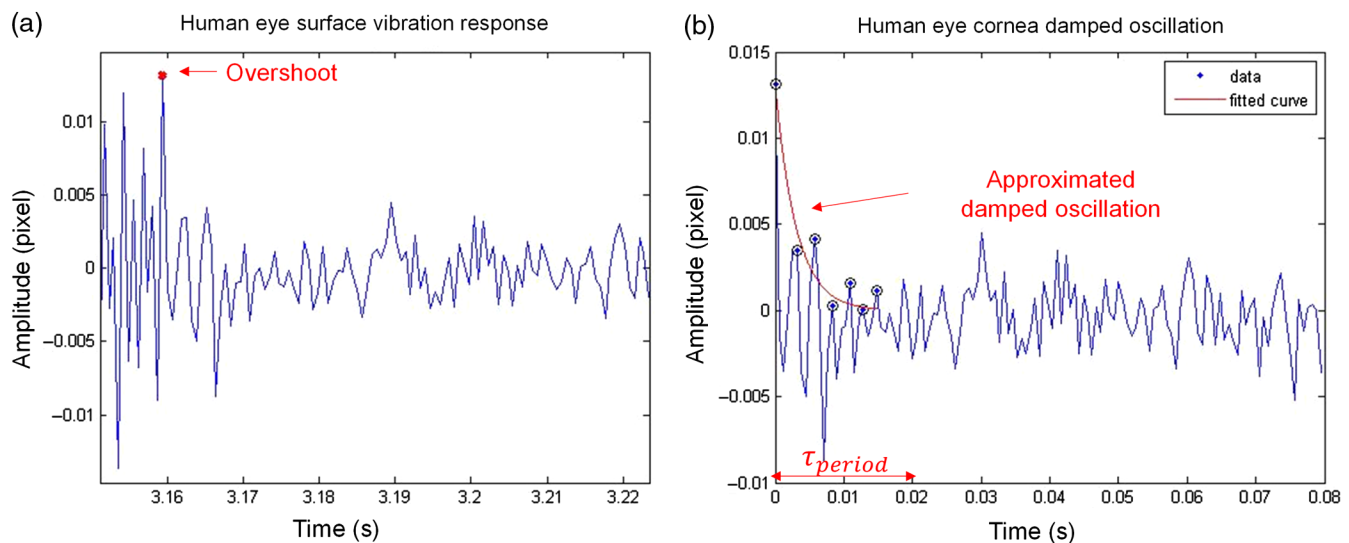


Fig. 9 Experimental results on human eyes. (a) The human eye vibration response signal and (b) human eye approximated damped oscillation.

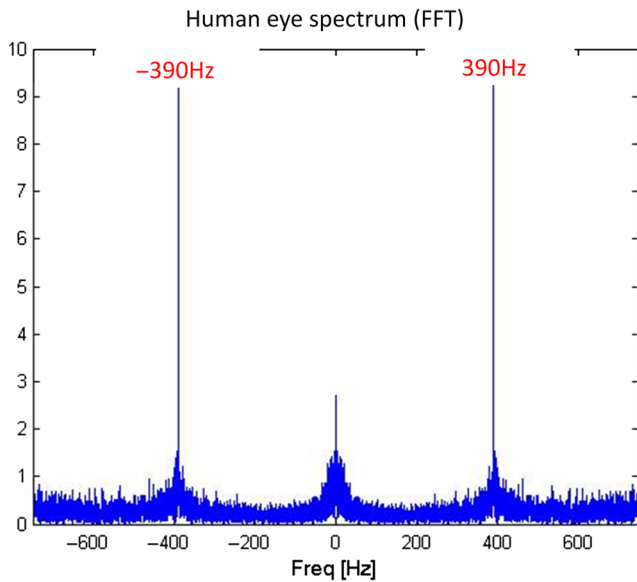


Fig. 10 The spectrum graph of the signal shown in Fig. 9. The 390-Hz excitation frequency is dominating on the graph.

the eye cornea, gave the best SNR after stimulation by sine sound waves at frequency of 390 Hz. The IOP was obtained by processing the reflected secondary speckle patterns of the stimulated artificial eye, fish eye, and human corneas when illuminated by a laser beam. We changed the concept of measurement by stimulating the eye with a temporally encoded external signal and after terminating the stimulation, observing transitional oscillation of the eye cornea for ~ 0.05 s. It was found that the accuracy of the artificial eye IOP measurement is about 1 mmHg within the range of pressures of 10 to 36 mmHg. Furthermore, we improved signal processing based on newly developed algorithms.

The speckle-based IOP measurement technique allows non-invasive semicontinuous monitoring by discrete frequent measurements, which is important for improved glaucoma diagnosis and management.

It should be noted that IOP measurements are also affected by corneal thickness and other biomechanical properties of the eye. At the present stage, preliminary calibration is required to improve the measurement precision. Future experiments will include investigation into the corneal thickness as a parameter in our IOP light-based measurement model.

The measurement also depends on proper alignment of the measuring instrument in relation to the illuminated object. For evaluation of human eyes IOP, further investigations are required due to the fact that such measurements produce noisy signals that need to be filtered and processed. Medical application of the device also requires its miniaturization and human friendly design.

The presented theoretical analyses show that phase shift between the agitation force and the output signal could be used for evaluation of the IOP. This will be the topic of our next study together with the factors mentioned above.

Disclosures

The authors have no financial interests in the manuscript and no other potential conflicts of interest to disclose. The invention described in the current research was submitted as an application for a patent to the USPTO.

References

1. H. A. Quigley, "Number of people with glaucoma worldwide," *Br. J. Ophthalmol.* **80**(5), 389–393 (1996).
2. G. L. Spaeth, "A new classification of glaucoma including focal glaucoma," *Surv. Ophthalmol.* **38**, S9–S17 (1994).
3. MayoClinic.org, *Mayo Clinic*, 2018, <http://www.mayoclinic.org/> (5 October 2016).
4. Nei.nih.gov, *National Eye Institute*, 2018, <https://nei.nih.gov/> (5 October 2016).
5. D. A. Lee and E. J. Higginbotham, "Glaucoma and its treatment: a review," *Am. J. Health-Syst. Pharm.* **62**(7), 691–699 (2005).
6. S. R. Flaxman et al., "Global causes of blindness and distance vision impairment 1990–2020: a systematic review and meta-analysis," *Lancet Global Health* **5**(12), e1221–e1234 (2017).
7. M. A. Kass et al., "The ocular hypertension treatment study: a randomized trial determines that topical ocular hypotensive medication delays or prevents the onset of primary open-angle glaucoma," *Arch. Ophthalmol.* **120**(6), 701–713 (2002).
8. P. R. Lichter et al., "Interim clinical outcomes in the collaborative initial glaucoma treatment study comparing initial treatment randomized to medications or surgery," *Ophthalmology* **108**(11), 1943–1953 (2001).
9. M. C. Leske et al., "Factors for glaucoma progression and the effect of treatment: the early manifest glaucoma trial," *Arch. Ophthalmol.* **121**(1), 48–56 (2003).
10. D. R. Anderson, S. M. Drance, and M. Schulzer, "Comparison of glaucomatous progression between untreated patients with normal-tension glaucoma and patients with therapeutically reduced intraocular pressures," *Am. J. Ophthalmol.* **126**(4), 487–497 (1998).
11. L. A. Ericson, "Twenty-four hourly variations in the inflow of the aqueous humour," *Acta Ophthalmol.* **36**(3), 381–385 (1958).
12. J. T. Wilensky, "Diurnal variations in intraocular pressure," *Trans. Am. Ophthalmol. Soc.* **89**, 757–790 (1991).
13. S. M. Drance, "The significance of the diurnal tension variations in normal and glaucomatous eyes," *Arch. Ophthalmol.* **64**(4), 494–501 (1960).
14. A. G. Konstas et al., "Effect of timolol on the diurnal intraocular pressure in exfoliation and primary open-angle glaucoma," *Arch. Ophthalmol.* **115**(8), 975–979 (1997).
15. J. H. Liu et al., "Twenty-four-hour pattern of intraocular pressure in the aging population," *Invest. Ophthalmol. Visual Sci.* **40**(12), 2912–2917 (1999).
16. P. L. Kaufman, "Diurnal fluctuation of intraocular pressure," *Invest. Ophthalmol. Visual Sci.* **57**(14), 6427–6427 (2016).
17. S. Srinivasan et al., "Diurnal intraocular pressure fluctuation and its risk factors in angle-closure and open-angle glaucoma," *Eye* **30**(3), 362–368 (2016).
18. H. A. N. S. Goldmann and T. H. Schmidt, "Über applanationstonometrie," *Ophthalmologica* **134**(4), 221–242 (1957).
19. D. M. Cockburn, "Tonometry," *Clin. Proced. Optometry* 221–237 (1991).
20. M. Shimmyo et al., "Intraocular pressure, Goldmann applanation tension, corneal thickness, and corneal curvature in Caucasians, Asians, Hispanics, and African Americans," *Am. J. Ophthalmol.* **136**(4), 603–613 (2003).
21. G. Rask and A. Behndig, "Effects of corneal thickness, curvature, astigmatism and direction of gaze on Goldmann applanation tonometry readings," *Ophthalmic Res.* **38**(1), 49–55 (2006).
22. S. Kaushik and S. S. Pandav, "Ocular response analyzer," *J. Curr. Glaucoma Pract.* **6**(1), 17–19 (2012).
23. T. Realini, "The ocular response analyzer," *J. Glaucoma Today* 27–30 (2008).
24. M. Zimmermann et al., "Tonographic effect of ocular response analyzer in comparison to goldmann applanation tonometry," *PLoS One* **12**(1), e0169438 (2017).
25. B. S. Uysal et al., "Impact of dehydration and fasting on intraocular pressure and corneal biomechanics measured by the ocular response analyzer," *Int. Ophthalmol.* **38**(2), 451–457 (2018).
26. W. W. Wang et al., "Study of noncontact air-puff applanation tonometry IOP measurement on irregularly-shaped corneas," *Proc. SPIE* **10251**, 102511X (2017).
27. R. Koprowski and S. Wilczyński, "Corneal vibrations during intraocular pressure measurement with an air-puff method," *J. Healthcare Eng.* **2018**, 1–13 (2018).

28. B. Grolman, "A new tonometer system," *Optom. Vision Sci.* **49**(8), 646–660 (1972).
29. J. W. McLaren, R. F. Brubaker, and J. S. FitzSimon, "Continuous measurement of intraocular pressure in rabbits by telemetry," *Invest. Ophthalmol. Visual Sci.* **37**(6), 966–975 (1996).
30. T. Kakaday et al., "Advances in telemetric continuous intraocular pressure assessment," *Br. J. Ophthalmol.* **93**(8), 992–996 (2009).
31. J. L. Hernández-Verdejo, "Simultaneous measurement of intraocular pressure in the anterior chamber and the vitreous cavity," *Acta Ophthalmol.* **88**(7), e265–e268 (2010).
32. K. Mansouri and T. Shaarawy, "Continuous intraocular pressure monitoring with a wireless ocular telemetry sensor: initial clinical experience in patients with open angle glaucoma," *Br. J. Ophthalmol.* **95**(5), 627–629 (2011).
33. B. Entenmann et al., "Contact lens tonometry—application in humans," *Invest. Ophthalmol. Visual Sci.* **38**(12), 2447–2451 (1997).
34. B. Mottet et al., "24-hour intraocular pressure rhythm in young healthy subjects evaluated with continuous monitoring using a contact lens sensor," *JAMA Ophthalmol.* **131**(12), 1507–1516 (2013).
35. K. Lorenz et al., "Tolerability of 24-hour intraocular pressure monitoring of a pressure-sensitive contact lens," *J. Glaucoma* **22**(4), 311–316 (2013).
36. K. Mansouri et al., "Analysis of continuous 24-hour intraocular pressure patterns in glaucoma," *Invest. Ophthalmol. Visual Sci.* **53**(13), 8050–8056 (2012).
37. K. Mansouri et al., "Continuous 24-hour monitoring of intraocular pressure patterns with a contact lens sensor: safety, tolerability, and reproducibility in patients with glaucoma," *Arch. Ophthalmol.* **130**(12), 1534–1539 (2012).
38. L. Agnifili et al., "Circadian intraocular pressure patterns in healthy subjects, primary open angle and normal tension glaucoma patients with a contact lens sensor," *Acta Ophthalmol.* **93**(1), e14–e21 (2015).
39. Y. Mandel, I. E. Araci, and S. R. Quake, "Implantable micro-fluidic device for monitoring of intra-ocular pressure," U.S. Patent Application 14/771, 576, Leland Stanford Junior University (2016).
40. S. De Smedt, A. Mermoud, and C. Schnyder, "24-hour intraocular pressure fluctuation monitoring using an ocular telemetry sensor: tolerability and functionality in healthy subjects," *J. Glaucoma* **21**(8), 539–544 (2012).
41. M. H. T. I. De, P. D. Ruiz, and J. M. Huntley, "Double-shot depth-resolved displacement field measurement using phase-contrast spectral optical coherence tomography," *Opt. Express* **14**(21), 9643–9656 (2006).
42. T. Matsumoto et al., "Measurement by holographic interferometry of the deformation of the eye accompanying changes in intraocular pressure," *Appl. Opt.* **17**(22), 3538–3539 (1978).
43. M. Asejczyk-Widlicka and B. K. Pierscionek, "Fluctuations in intraocular pressure and the potential effect on aberrations of the eye," *Br. J. Ophthalmol.* **91**(8), 1054–1058 (2007).
44. P. Dubois et al., "A new method for intra ocular pressure in vivo measurement: first clinical trials," in *29th Annual Int. Conf. of the IEEE Engineering in Medicine and Biology Society, IEEE*, pp. 5762–5765 (2007).
45. J. L. Zuckerman and H. J. Grossman, "Method of measuring ocular pulse," U.S. Patent 3, 948, 248 (1976).
46. B. I. Akca et al., "Observation of sound-induced corneal vibrational modes by optical coherence tomography," *Biomed. Opt. Express* **6**(9), 3313–3319 (2015).
47. Z. Zalevsky et al., "Simultaneous remote extraction of multiple speech sources and heart beats from secondary speckles pattern," *Opt. Express* **17**(24), 21566–21580 (2009).
48. Z. Zalevsky and J. Garcia, "Motion detection system and method," U.S. Patent 8, 638, 991, Universitat de Valencia and Bar Ilan University (2014).
49. Y. Beiderman et al., "Use of PC mouse components for continuous measuring of human heartbeat," *Appl. Opt.* **51**(16), 3323–3328 (2012).
50. Y. Beiderman et al., "Remote estimation of blood pulse pressure via temporal tracking of reflected secondary speckles pattern," *J. Biomed. Opt.* **15**(6), 061707 (2010).
51. A. Bennett et al., "Approach to breast cancer early detection via tracking of secondary speckle patterns reflected from the skin with artificial intradermal impurity," *Biomed. Opt. Express* **8**(12), 5359–5367 (2017).
52. Y. Beiderman et al., "Demonstration of remote optical measurement configuration that correlates to glucose concentration in blood," *Biomed. Opt. Express* **2**(4), 858–870 (2011).
53. N. Ozana et al., "Improved noncontact optical sensor for detection of glucose concentration and indication of dehydration level," *Biomed. Opt. Express* **5**(6), 1926–1940 (2014).
54. I. Margalit et al., "New method for remote and repeatable monitoring of intraocular pressure variations," *J. Biomed. Opt.* **19**(2), 027002 (2014).
55. Y. Beiderman et al., "Optical remote continuous sensing of intraocular pressure variations," *Proc. SPIE* **8209**, 820908 (2012).
56. T. Miwa, "Non-contact ultrasonic tonometer," United States patent application US 12/817, 850, Nidek Co. Ltd. (2010).
57. H. Hsu, "Non-contact high frequency tonometer," U.S. Patent 4, 928, 697, Ohio State University (1990).
58. Feynmanlectures.caltech.edu, "The Feynman lectures on physics," 2018, <http://www.feynmanlectures.caltech.edu/> (8 December 2016).

Aviya Bennett received her BSc and MSc degrees in electrical engineering from Bar-Ilan University (BIU) in 2005 and 2016, respectively. In between, she worked at Intel Electronics Corporation. Currently, she is working toward her PhD studies under Prof. Zeev Zalevsky's supervision. She received the "Intel prize for Academic Excellence" in 2015. Her research interests include optical remote sensing, biomedical optics, and nanophotonics. She has published three refereed journal papers.

Sergey Agdarov received his MSc degree in mechanics and mathematics from Tajiki State University of Dushanbe, Tajikistan, in 1987. Since 2011, he has worked as a researcher in the faculty of engineering at Bar-Ilan University, Ramat-Gan, Israel. His research involves the development, testing and evaluation of biomedical optical sensors, non-invasive measurement of IOP, breast cancer early detection, silicon-based mechanic-photonic wavelength conversion, fiber sensors for non-contact estimation of vital bio-signs.

Yafim Beiderman received his MSc degree in mechanics from the Polytechnic Institute, Odessa, Ukraine, his PhD from agricultural academy, Latvia. From 2015, he is with Bar-Ilan University, Israel. His research involves the development, testing and evaluation of biomedical sensors, non-invasive laser speckle-based measurement of blood and intra-ocular pressure, breast cancer early detection, fiber based non-contact estimation of vital bio-signs, and alternative ways for information transmission to the brain of blind people.

Nisan Ozana received a BSc degree in electrical engineering from Bar-Ilan University, Ramat Gan, Israel, in 2013 and his MSc degree in electrical engineering from Bar-Ilan University in 2015. Currently, he is working toward his PhD at Bar-Ilan University, where he is supervised by Prof. Zalevsky. He has received several awards for his research activity, such as a Wolf Foundation prize for outstanding PhD students and Prize4Life for developing assistive technology for ALS patients. His research interests include extraction and separation of remote vibration sources, optical remote sensing, biomedical optics, nanophotonics and neuroscience. He has published 14 refereed journal papers, 17 conference proceeding papers, and has seven patents pending.

Zeev Zalevsky received his BSc and direct PhD degrees in electrical engineering from Tel-Aviv University in 1993 and 1996, respectively. Currently, he is a full professor in the faculty of engineering at Bar-Ilan University, Israel. He is the vice dean of engineering, the head of the electro-optics track and the director of the nano photonic center there. His major fields of research are optical super-resolution, biomedical optics, nano-photonics, electro-optical devices, and microwave photonics. He has published more than 700 papers, 9 books, and has more than 100 patents.

Biographies for the other authors are not available.